Original Article

Correlation between Peripapillary Atrophy and Optic Nerve Head Blood Flow in Eyes with Untreated Normal-Tension Glaucoma

Hiroyuki Ito*   Tetsuro Takumi   Nobuko Enomoto
Ayako Anraku   Kyoko Ishida and Goji Tomita

Department of Ophthalmology, Toho University, Ohashi Medical Center, Tokyo, Japan

ABSTRACT

Introduction: To evaluate relationships between the area and extent of peripapillary atrophy (PPA) and optic nerve head (ONH) blood flow and between PPA parameters and structural and functional damage in eyes with untreated normal-tension glaucoma (NTG).

Methods: Thirty-six eyes (36 subjects) with newly diagnosed, untreated NTG were included. Correlations between PPA and ONH blood flow were examined. The PPA was examined using confocal scanning laser ophthalmoscopy, ONH was examined using laser speckle flowgraphy, and circumpapillary retinal nerve fiber layer thickness was measured using spectral-domain optical coherence tomography. Retinal function was examined using standard automated perimetry mean deviation (MD).

Results: The PPA area was significantly correlated with the refractive spherical equivalent ($r = -0.418$, $P = 0.010$), mean blur rate (MBR) inside the ONH (MBR$_A$; $r = -0.394$, $P = 0.016$), and MBR of ONH tissue (MBR$_T$; $r = -0.328$, $P = 0.048$). Total angular extent around the ONH of PPA was significantly correlated with MD ($r = -0.344$, $P = 0.037$), MBR$_A$ ($r = -0.360$, $P = 0.029$), and MBR$_T$ ($r = -0.368$, $P = 0.025$). Multiple regression analyses revealed that PPA area significantly contributed to changes in MBR$_A$. Total angular extent of PPA significantly contributed to changes in MBR$_T$.

Conclusions: Significant relationships between PPA and ONH blood flow parameters were identified in eyes with untreated NTG.

Toho J Med 4 (4): 123–131, 2018

KEYWORDS: glaucoma, peripapillary atrophy, laser speckle flowgraphy

Introduction

Peripapillary atrophy (PPA) is one of the most common structural changes that occur during the development and progression of glaucomatous optic nerve head (ONH) damage.[1-6] In fact, PPA was observed in 87% of glaucomatous eyes, but in only 30% of normal eyes in a Japanese population.[7, 8] Cross-sectional studies have shown that PPA extent and location, especially β-zone PPA, were significantly correlated with glaucomatous ONH damage[5, 6, 9-11] and visual field defects[5, 6, 10, 12, 13] in eyes with primary open-angle glaucoma (POAG). In addition, longitudinal studies[14-16] and

retrospective cohort studies[17, 18] suggest that the presence and extent of β-zone PPA are predictive of visual field deterioration in eyes with POAG. The β-zone PPA is defined as an area of visible sclera adjacent to the clinically visible optic disc margin, corresponding to an area without retinal pigment epithelium.[4] The β-zone PPA is further divided into two subsets that are indistinguishable by clinical examination: an area with intact Bruch's membrane, still termed β-zone PPA, and an area lacking Bruch's membrane, termed γ-zone PPA.[19]

The β-zone PPA does not fluoresce during fluorescein angiography in the choroidal filling phase.[20] Histologically, areas that do not fluoresce are regions with thinning or no choroid[17] and areas next to the disc with no retinal pigment epithelium.[17, 21, 22] The prelaminar ONH mainly receives its blood supply from the peripapillary choroid via branches of the short posterior ciliary arteries. Therefore, it has a characteristic sectoral distribution[23–26] and the absence or dysfunction of a centripetal branch will cause ischemic ONH damage in the corresponding PPA sector.[25, 26] Previous reports have shown that visual field defects and ONH damage correlate with PPA location.[27–29] Thus, regional PPA may be representative of a local vascular insufficiency in the corresponding ONH segment[1, 30] and may be a local vascular risk factor for the development of glaucomatous ONH damage.

Few studies have directly examined the relationship between PPA and ONH blood flow.[31] Therefore, the aim of the present study was to evaluate relationships between the clinically assessed area and extent of the β-zone PPA (including γ-zone PPA) and ONH blood flow. Eyes with normal-tension glaucoma (NTG) that were not being treated with eye drops for glaucoma were examined to eliminate influences of medication on ocular blood flow as much as possible. Structural glaucomatous damage was evaluated using spectral-domain optical coherence tomography (SD-OCT) measurements of circumpapillary retinal nerve fiber layer (cpRNFL) thickness. Functional glaucomatous damage was also examined using Humphrey visual field testing results.

Materials and Methods

This study protocol was reviewed and approved by the Ethics Committee of Toho University Ohashi Medical Center (No. 12-82). All study conduct adhered to the tenets of the Declaration of Helsinki, and all subjects provided written informed consent. Before providing this consent, all subjects had been thoroughly explained of the study purposes and methods.

Study participants

Subjects that had been newly diagnosed with NTG and who had not been treated with medication were considered for enrollment in this prospective, cross-sectional study. All subjects were enrolled between December 2012 and December 2015 at the Department of Ophthalmology, Toho University Ohashi Medical Center (Tokyo, Japan). Subjects were included in the study if all of the following were true: visual acuity was at least 20/25, refractive spherical equivalent (SE) was within ± 6.0 D, anterior chamber angles were normal and open (determined with slit-lamp biomicroscopy and gonioscopy), intraocular pressure (IOP) was < 22 mmHg (determined with repeated Goldmann applanation tonometry measurements over a 24 h period), reproducible and reliable visual field testing (fixation error < 20%, false-positive/negative error < 20%), and a glaucomatous visual field defect was present (30-2 SITA Standard testing, Humphrey Field Analyzer [HFA], Carl Zeiss Meditec, Dublin, CA). Subjects were excluded if any other fundus abnormalities or media opacities (except mild cataract) were detected. This included a history of intraocular surgery, the presence of intraocular disease known to affect image quality or visual field testing results (e.g., diabetic retinopathy or age-related macular degeneration), a history of systemic disease known to affect IOP and/or visual field testing results (e.g., intracranial disease and steroid use). If both eyes were eligible, one eye was randomly chosen as the study eye.

Subjects had originally been diagnosed with glaucoma based on glaucomatous optic disc and/or RNFL changes and a corresponding visual field defect. Glaucomatous fundus changes included an enlarged vertical cup-to-disc ratio, rim width thinning, and/or an RNFL defect. A glaucomatous visual field defect was defined as the presence of at least one of the following Anderson and Patella[32] criteria: pattern deviation probability plot with ≥3 points not on the edge with a < 5% probability and at least one point with a < 1% probability in an expected location, a pattern standard deviation (SD) with a < 5% probability, or a glaucoma hemifield test that indicated a field outside normal limits.

Study examinations

All subjects underwent a complete ophthalmological examination and assessment of medical and family histories. Ophthalmological examination included visual acuity test-
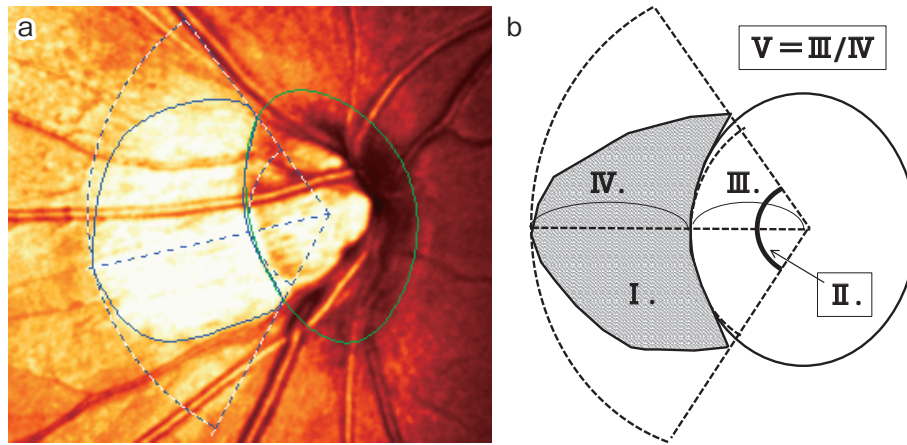
Fig. 1 Measurement of peripapillary atrophy (PPA) parameters. Morphometry of β-zone PPA was defined as a region of chorioretinal atrophy with visible sclera and choroidal vessels adjacent to the optic nerve head (ONH). Parameters were measured using the Heidelberg Retinal Tomograph 3 (HRT3) PPA analysis program. An HRT3 image is shown (a) with corresponding HRT3 PPA analyses (b). The program automatically calculated atrophy area (mm², I), total angular extent around the ONH (degrees, II), total radial extent from the ONH center (mm, III), maximum distance from the ONH edge (mm, IV), and the ratio of maximum distance from contour to the ONH radius (Max distance/radius, V).

ing (including refraction using an autorefractometer (RK-5; Canon, Tokyo, Japan)), slit-lamp biomicroscopy, gonioscopy, Goldmann applanation tonometry, and dilated stereoscopic fundus examination. In addition, all subjects underwent confocal scanning laser ophthalmoscopy (Heidelberg Retinal Tomograph 3 [HRT 3], Heidelberg Engineering GmbH, Dossenheim, Germany) to measure PPA parameters, SD-OCT (RTVue-100, software ver. 4.0, Optovue, Inc., Fremont, CA) to measure cpRNFL thickness, and standard automated perimetry (SAP; HFA) to examine visual field defects. Laser speckle flowgraphy (LSFG; Softcare, Iizuka, Japan) was also used to examine ONH blood flow. Visual field parameters, PPA measurements, cpRNFL thickness measurements, and ONH blood flow were obtained within an interval of <3 months.

Confocal scanning laser ophthalmoscopy

The PPA parameters were evaluated using the HRT3 system (software version 33.1.2.4) with a diode laser (670 nm wavelength) for sequential scanning of the retinal surface in the horizontal and vertical directions in multiple focal planes.[10, 13, 29] Using confocal scanning principles, a three-dimensional topographic image was constructed from a series of 384 × 384 pixel (147,456-pixel) optical image sections, with each pixel corresponding to the retinal height at its corresponding location. The optic disc contour line was drawn along the inner margin of the scleral ring.

A reference plane was automatically set 50 μm posterior to the mean height of the disc margin contour line in a temporal segment between 350° and 356°. All study images were obtained through dilated pupils with a 15° field-of-view, and PPA parameters were measured in the β-zone. The β-zone PPA was defined as a region of chorioretinal atrophy with visible sclera and choroidal vessels adjacent to the ONH. To evaluate PPA parameters, a new contour line was drawn on the HRT3 ONH image to delineate the β-zone PPA (Fig. 1). The built-in PPA analysis program then calculated atrophy area (mm²), total angular extent around the ONH (total angular extent, degrees), total radial extent from the ONH center (total radial extent, mm), maximum distance from the ONH edge (max distance from contour, mm), and the ratio of the maximum distance from contour to the ONH radius (max distance radius, Fig. 1).

All measurements were performed by a well-trained operator. Data with an average SD >30 μm and images with unacceptable or poor quality were excluded from analyses. The HRT corrects for most magnification errors so that the mean residual error is −1.3-2.0% compared with an axial length derived standard.[33]

Laser speckle flowgraphy

A LSFG device was used to measure mean blur rate (MBR), an indicator of blood flow,[34, 35] in the ONH. The prin-
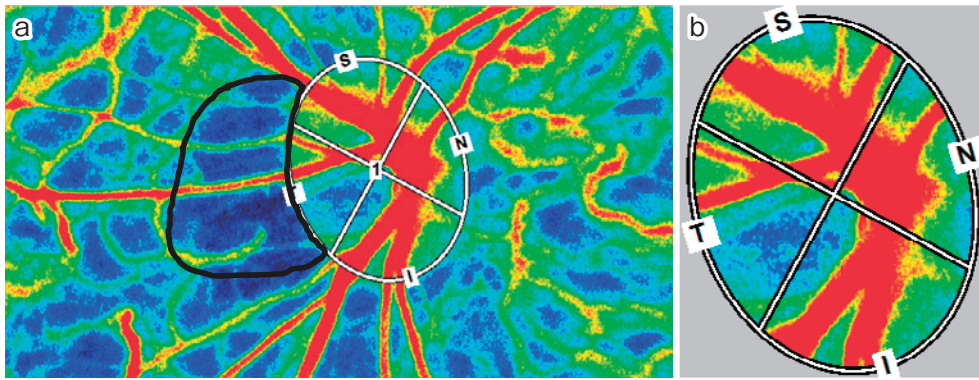
Fig. 2 Evaluation of optic nerve head (ONH) blood flow. Laser speckle flowgraphy (LSFG) was used to measure mean blur rate (MBR), an indicator of blood flow. The LSFG system defined an area centered on the ONH. A speckle pattern was created by random interference of scattered light reflected from the illuminated area and was displayed as an MBR image (a). An area surrounded by the black line indicates β-zone PPA. The MBR was continuously imaged by a charge coupled device. Optic disc edges were manually marked on the image, and disc edge location was saved in system software. Vessels were then automatically segmented using an automated defining threshold. Values of mean MBR (MBR_A), vessel area MBR (MBR_V), and tissue area MBR (MBR_T) were determined in the whole disc and superior (S), nasal (N), inferior (I), and temporal (T) quadrants (b).

ciples of and methods to obtain ONH blood flow measurements using LSFG have been previously described.[34–37] Briefly, a fundus camera-based LSFG device was used to define a 3.8 × 3.0 mm area (width × height) centered on the ONH that was used to measure blood flow up to an estimated tissue penetration depth of approximately 1 mm (laser λ = 810 nm). After switching on the laser (λ = 830 nm, maximum output power = 1.2 mW), a speckle pattern appeared because of random interference of scattered light from the illuminated area. This light was continuously imaged by a charge coupled device (700 × 480 pixel) at a frequency of 30 frames/s. All LSFG images were obtained through a dilated pupil (0.4% tropicamide, Midrin-M, Santen Pharmaceutical Co. Ltd., Osaka, Japan).

Subjects rested on a chair with their eyes closed for 10 min in a dark room before LSFG examination and blood pressure measurement. All examinations were performed by a single experienced operator. Optic disc edge detection in MBR images was manually marked on the image, and the disc edge location was saved by the software. Vessels were then automatically segmented by system software (LSFG Analyzer, ver. 3.0.47.0) using an automated defining threshold. Values of mean MBR (MBR_A), MBR in the vessel area (MBR_V), and MBR in the tissue area (MBR_T) were provided (Fig. 2). All measurements were repeated three times for each subject, with individual measurements taken several minutes apart. Parameters were de-

termined using saved data for the optic disc edge, and the means of the three individual measurements were used in study analyses. We considered MBR_A and MBR_T represent the ONH blood flow and used for further analyses.

Spectral-domain optical coherence tomography

All SD-OCT images were obtained with the RTVue-100 system for cpRNFL thickness measurement. The SD-OCT uses a scanning laser diode that emits a beam with a wavelength of 840±10 nm to provide images of ocular microstructures. In this study, the ONH protocol was used to measure cpRNFL thickness. The total time to acquire a single scan was 0.55 s. Using the SD-OCT-generated fundus image (video baseline protocol), we manually traced the ONH contour. Using the ONH scanning protocol software, the RNFL thickness was automatically measured along a 3.45 mm diameter circle centered on the optic disc using a total of 775 A-scans. The scan circle did not pass over areas with PPA. The cpRNFL thickness parameter represents the mean of all measurements made over the entire 360° circle. Measurements were performed by a well-trained operator, and images with signal strength index (SSI) ＜30 were excluded from analyses.

Statistical analyses

Data are reported as mean±SD. Pearson's correlation coefficients were used to examine correlations between PPA parameters and MBR_A, MBR_T, SAP mean deviation (MD), cpRNFL, and clinical factors. All statistical analyses

Table 1 Demographic and clinical characteristics of study subjects.

Variable	Total (n = 36 eyes/patients)
Sex (male/female)	12/24
Age (years)	57.64 ± 12.67 (34-79)
Refractive errors in the spherical equivalent (D)	−2.38 ± 2.49 (−5.75-2.25)
IOP (mmHg)	15.21 ± 3.00 (10.00-21.00)
MD (dB)	−4.53 ± 4.61 (−23.95-0.30)
cpRNFL thickness (μm)	78.24 ± 10.61 (58.00-100.98)
PPA parameters:	
Atrophy area (mm²)	0.88 ± 0.53 (0.00-1.98)
Total angular extent (degrees)	151.86 ± 59.37 (0.00-324.43)
Total radial extent (mm)	0.53 ± 0.24 (0.00-1.00)
Max distance from contour (mm)	0.49 ± 0.25 (0.00-0.99)
Max distance radius	0.70 ± 0.45 (0.00-1.73)
MA	20.73 ± 5.01 (8.16-30.78)
MT	10.47 ± 2.93 (4.54-16.83)

Data are presented as mean ± standard deviation (range). Total angular extent was defined as the total angular extent around the optic nerve head (ONH). Total radial extent was defined as the total radial extent from the ONH center. Max distance from contour was defined as the maximum distance from the ONH edge. Max distance radius was defined as the ratio of maximum distance from contour to the ONH radius. IOP: intraocular pressure, cpRNFL: circumpapillary retinal nerve fiber layer, MD: mean deviation, PPA: peripapillary atrophy, MA: mean blur rate inside the ONH, MT: mean blur rate in the ONH tissue.

were performed using SPSS statistical software (version 20.0; SPSS, Inc., Chicago, IL), and statistical significance was defined as $P < 0.05$.

Results

In total, 36 eyes of 36 subjects with newly diagnosed, treatment-naïve NTG were included in this study. Of 36 eyes, one eye did not have PPA. Five subjects were treated with internal medicines for their systemic hypertension. However, no subjects received other internal medicines such as statins nor were smoking. Table 1 summarizes subject characteristics at the time of enrollment.

Pearson's correlation coefficients for relationships between each PPA parameter and age, refraction, IOP at the time of LSFG, MT, cpRNFL thickness, and MD are summarized in Table 2. The atrophy area was significantly correlated with refractive SE ($r = -0.418$, $P = 0.010$), cpRNFL ($r = -0.336$, $P = 0.042$), MBR$_A$ ($r = -0.394$, $P = 0.016$), and MBR$_T$ ($r = -0.328$, $P = 0.048$). Total angular extent was significantly correlated with MD ($r = -0.344$, $P = 0.037$), MBR$_A$ ($r = -0.360$, $P = 0.029$), and MBR$_T$ ($r = -0.368$, $P = 0.025$). Total radial extent ($r = -0.415$, $P = 0.011$), max distance from contour ($r = -0.408$, $P = 0.012$), and max dis-

tance radius ($r = -0.431$, $P = 0.008$) were all significantly correlated with refractive SE (Fig. 3) .

Multiple regression analyses were performed using the stepwise method (a combination of backward and forward methods), where MBR$_A$ or MBR$_T$ was used as the dependent variable and age, refraction, IOP, cpRNFL thickness, MD, and PPA parameters were used as explanatory variables. Consequently, atrophy area (partial correlation coefficient [r] = −0.410, standard partial regression coefficient [β] = −0.410, 95% confidence interval (CI) = −6.839-−0.867, $P = 0.013$) significantly contributed to variations in MBR$_A$ only. Also, only total angular extent (r = −0.434, β = −0.434, 95% CI = −0.037-−0.006, $P = 0.008$) significantly contributed to variations in MBR$_T$ (Table 3).

Discussion

Here, we investigated relationships between PPA parameters (area and extent), ONH tissue blood flow, glaucomatous structural damage, and glaucomatous functional deficits in newly diagnosed, treatment-naïve eyes with NTG. To do this, cpRNFL thickness was measured using SD-OCT and visual field defects were examined using the HFA. Our study showed that atrophy area was signifi-

Table 2   Correlations of PPA parameters with clinical factors.

PPA parameters \ Factors	Age	Refractive error	IOP	MD	cpRNFL thickness	MBR$_A$	MBR$_T$
Atrophy area	−0.036 (0.833)	**−0.418 (0.010)**	0.169 (0.318)	−0.323 (0.051)	**−0.336 (0.042)**	**−0.394 (0.016)**	**−0.328 (0.048)**
Total angular extent	0.113 (0.504)	−0.171 (0.311)	0.134 (0.429)	**−0.344 (0.037)**	−0.276 (0.099)	**−0.360 (0.029)**	**−0.368 (0.025)**
Total radial extent	−0.193 (0.251)	**−0.415 (0.011)**	0.134 (0.428)	−0.315 (0.057)	−0.253 (0.131)	−0.267 (0.110)	−0.151 (0.374)
Max distance from contour	−0.226 (0.180)	**−0.408 (0.012)**	0.124 (0.463)	−0.242 (0.149)	−0.241 (0.151)	−0.248 (0.139)	−0.123 (0.469)
Max distance radius	−0.241 (0.150)	**−0.431 (0.008)**	0.055 (0.748)	−0.233 (0.165)	**−0.351 (0.033)**	−0.304 (0.067)	−0.136 (0.423)

Data are presented as Pearson's correlation coefficient (P-value). Total angular extent was defined as the total angular extent around the optic nerve head (ONH). Total radial extent was defined as the total radial extent from the ONH center. Max distance from contour was defined as the maximum distance from the ONH edge. Max distance radius was defined as the ratio of maximum distance from contour to the ONH radius. IOP: intraocular pressure, cpRNFL: circumpapillary retinal nerve fiber layer, MD: mean deviation, PPA: peripapillary atrophy, MBR$_A$: mean blur rate inside the ONH, MBR$_T$: mean blur rate in ONH tissue.
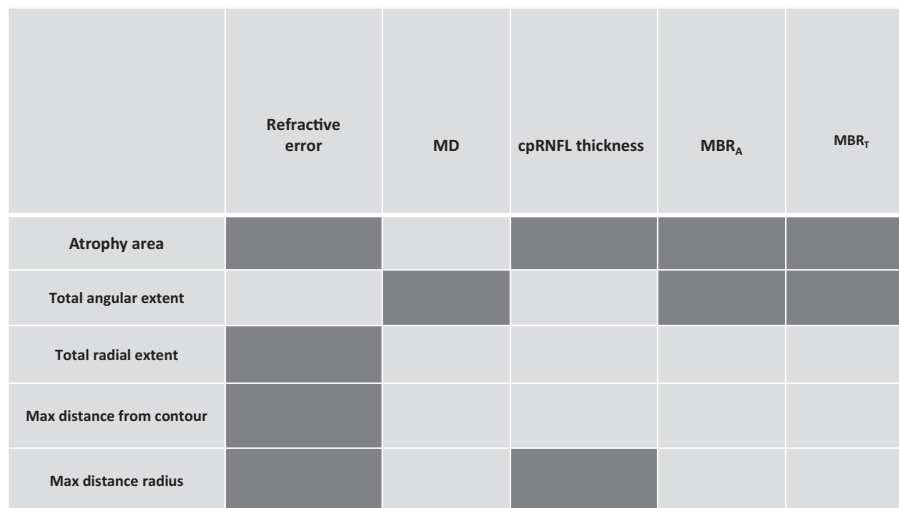
: Significant correlation

Fig. 3   Correlation diagram between PPA parameters and other factors including optic nerve head flow. Dark gray color indicates a significant correlation ($P < 0.05$) between the factors. Total angular extent was defined as the total angular extent around the optic nerve head (ONH). Total radial extent was defined as the total radial extent from the ONH center. Max distance from contour was defined as the maximum distance from the ONH edge. Max distance radius was defined as the ratio of maximum distance from contour to the ONH radius. PPA: peripapillary atrophy, cpRNFL: circumpapillary retinal nerve fiber layer, MD: mean deviation, MBR$_A$: mean blur rate inside the ONH, MBR$_T$: mean blur rate in ONH tissue.

cantly correlated with refractive SE and overall (MBR$_A$) and tissue (MBR$_T$) ONH blood flow. Total angular extent was significantly correlated with visual field (MD) and ONH blood flow (MBR$_A$ and MBR$_T$). The other three parameters were only correlated with refractive SE. Multiple regression analyses revealed that PPA area significantly contributed to variations in MBR$_A$ only. Also, total angular extent around the ONH of PPA was the only parameter that significantly contributed to variations in MBR$_T$.

Table 3 Multiple regression analyses between optic nerve head tissue mean blur rate (MBR$_T$) and other examined factors.

	r	SE	β	95% CI	P-value
Total angular extent of PPA	−0.434	0.008	−0.434	−0.037- −0.006	0.008

The dependent variable was MBR$_T$, and explanatory variables were age, refractive spherical equivalent, intraocular pressure (IOP), circumpapillary retinal nerve fiber layer (cpRNFL) thickness, standard automated perimetry mean deviation (MD), and peripapillary atrophy (PPA) parameters. r: partial correlation coefficient, SE: standard error, β: standardized partial regression coefficient, CI: confidence interval.

Many studies have reported a significant relationship between PPA and glaucoma and a relationship between ONH blood flow and glaucoma.[38, 39] However, the factors that influence PPA and ONH tissue blood flow are poorly understood. The present study showed that PPA parameters, particularly area and angular extent around the ONH, were significantly correlated with ONH blood flow. However, PPA is frequently observed in the temporal side of the ONH. Thus, the reason why the PPA located in the temporal side of the ONH correlated with the whole ONH blood flow is unclear. One possible explanation is that at least MBR$_T$ (tissue blood flow of the whole ONH) may have reflected mainly the tissue blood flow in the temporal side of the ONH, because the ONH vessels usually tend to shift to the nasal side of the ONH in glaucomatous eyes.

Previous studies have also shown that PPA is related to myopic ONH changes.[40] In the current study, univariate linear regression analyses revealed that all PPA parameters were significantly correlated with refractive SE, except for total angular extent. Myopic changes related to PPA are usually limited to the temporal side of the ONH (i.e., temporal conus), but PPA may have extended over the superior or inferior pole of the ONH because of glaucomatous changes. This theory is supported by the finding that total angular extent was also significantly correlated with SAP MD. In addition, multiple regression analysis revealed that PPA area and total angular extent contributed to variations in ONH tissue blood flow. This finding may also indicate that PPA in our subjects was mainly related to ONH blood flow abnormalities associated with glaucoma. However, because the correlation was relatively weak (Pearson's correlation coefficient was approximately 0.4), it remains unclear whether or not PPA directly affects ONH blood flow and leads to glaucoma progression. However, at the very least, PPA seems to indicate a decrease in ONH blood flow in eyes with untreated NTG.

Previous studies[10, 11, 13] have shown significant correlations between PPA parameters and glaucomatous functional and structural changes. For unknown reasons, we only found a weak relationship between these parameters. One possible explanation is that, unlike previous reports, we examined newly diagnosed, treatment-naïve eyes with NTG. Additionally, although there were 4 eyes those had MD value < −10 dB, mean visual field MD of our subjects can be considered as early stage (mean visual field MD = −4.53 ± 4.61 dB). Therefore, our relatively, early-stage glaucoma subjects may have had a different amount of glaucomatous damage than subjects examined in previous studies.

Our study had several limitations. First, the number of subjects enrolled was relatively small, which likely resulted from the fact we selected NTG patients who were not receiving treatment for glaucoma. In our ophthalmology clinic at a university hospital, nearly all patients referred for glaucoma are treated. Second, we examined β-zone PPA using HRT3 images, which may have also included γ-zone PPA.[19] Although γ-zone PPA is thought to be correlated with axial globe elongation, we excluded highly myopic eyes from this study. Still, further investigations that carefully exclude imaging γ-zone PPA are needed.

In conclusion, we demonstrated a direct relationship between PPA parameters and ONH blood flow for the first time in treatment-naïve eyes with NTG. PPA can be an indicator suggesting ONH blood flow decrease. However, further studies are needed to clarify a role of PPA in decreasing ONH blood flow.

Conflicts of interest: The authors declare no conflicts of interest

References

1) Primrose J. Early signs of the glaucomatous disc. Br J Ophthalmol. 1971; 55: 820-5.

2) Wilensky JT, Kolker AE. Peripapillary changes in glaucoma. Am J Ophthalmol. 1976; 81: 341-5.

3) Geijssen HC, Greve EL. The spectrum of primary open angle glaucoma. I: Senile sclerotic glaucoma versus high tension glaucoma. Ophthalmic Surg. 1987; 18: 207-13.

4) Jonas JB, Nguyen XN, Gusek GC, Naumann GO. Parapapillary chorioretinal atrophy in normal and glaucoma eyes. I. Morphometric data. Invest Ophthalmol Vis Sci. 1989; 30: 908-18.

5) Jonas JB, Naumann GO. Parapapillary chorioretinal atrophy in normal and glaucoma eyes. II. Correlations. Invest Ophthalmol Vis Sci. 1989; 30: 919-26.

6) Jonas JB, Fernandez MC, Naumann GO. Glaucomatous parapapillary atrophy. Occurrence and correlations. Arch Ophthalmol. 1992; 110: 214-22.

7) Sugiyama K, Tomita G, Kawase K, Onda E, Shinohara H, Hayakawa T, et al. Disc hemorrhage and peripapillary atrophy in apparently healthy subjects. Acta Ophthalmol Scand. 1999; 77: 139-42.

8) Hayakawa T, Sugiyama K, Tomita G, Kawase K, Onda E, Shinohara H, et al. Correlation of the peripapillary atrophy area with optic disc cupping and disc hemorrhage. J Glaucoma. 1998; 7: 306-11.

9) Tezel G, Kass MA, Kolker AE, Wax MB. Comparative optic disc analysis in normal pressure glaucoma, primary open-angle glaucoma, and ocular hypertension. Ophthalmology. 1996; 103: 2105-13.

10) Park KH, Tomita G, Liou SY, Kitazawa Y. Correlation between peripapillary atrophy and optic nerve damage in normal-tension glaucoma. Ophthalmology. 1996; 103: 1899-906.

11) Resch H, Schmidl D, Hommer A, Rensch F, Jonas JB, Fuchsjäger-Mayrl G, et al. Correlation of optic disc morphology and ocular perfusion parameters in patients with primary open angle glaucoma. Acta Ophthalmol. 2011; 89: e544-9.

12) Jonas JB, Gründler AE. Correlation between mean visual field loss and morphometric optic disk variables in the open-angle glaucomas. Am J Ophthalmol. 1997; 124: 488-97.

13) Kono Y, Zangwill L, Sample PA, Jonas JB, Emdadi A, Gupta N, et al. Relationship between parapapillary atrophy and visual field abnormality in primary open angle glaucoma. Am J Ophthalmol. 1999; 127: 674-80.

14) Tezel G, Kolker AE, Kass MA, Wax MB, Gordon M, Siegmund KD. Parapapillary chorioretinal atrophy in patients with ocular hypertension, I. An evaluation as a predictive factor for the development of glaucomatous damage. Arch Ophthalmol. 1997; 115: 1503-8.

15) Araie M, Sekine M, Suzuki Y, Koseki N. Factors contributing to the progression of visual field damage in eyes with normal tension glaucoma. Ophthalmology. 1994; 101: 1440-4.

16) Uchida H, Ugurlu S, Caprioli J. Increasing peripapillary atrophy is associated with progressive glaucoma. Ophthalmology. 1998; 105: 1541-5.

17) Fantes FE, Anderson DR. Clinical histologic correlation of human peripapillary anatomy. Ophthalmology. 1989; 96: 20-5.

18) Curcio CA, Saunders PL, Younger PW, Malek G. Peripapillary chorioretinal atrophy: Bruch's membrane changes and photoreceptor loss. Ophthalmology. 2000; 107: 334-43.

19) Jonas JB, Jonas SB, Jonas RA, Holbach L, Dai Y, Sun X, et al. Parapapillary atrophy: histological gamma zone and delta zone. PLoS ONE. 2012; 7: e47237.

20) Hayreh SS, Walker WM. Fluorescent fundus photography in glaucoma. Am J Ophthalmol. 1967; 63: 982-9.

21) Kubota T, Jonas JB, Naumann GO. Direct clinico-histological correlation of parapapillary chorioretinal atrophy. Br J Ophthalmol. 1993; 77: 103-6.

22) Jonas JB, Königsreuther KA, Naumann GO. Optic disc histomorphometry in normal eyes and eyes with secondary angle-closure glaucoma. II. Parapapillary region. Graefes Arch Clin Exp Ophthalmol. 1992; 230: 134-9.

23) Lieberman MF, Maumenee AE, Green WR. Histologic studies of the vasculature of the anterior optic nerve. Am J Ophthalmol. 1976; 82: 405-23.

24) Anderson DR, Braverman S. Reevaluation of optic disk vasculature. Am J Ophthalmol. 1976; 82: 165-74.

25) Hayreh SS. Blood supply of the optic nerve head and its role in optic atrophy, glaucoma, and oedema of the optic disc. Br J Ophthalmol. 1969; 53: 721-48.

26) Hayreh SS. The 1994 Von Sallman Lecture. The optic nerve head circulation in health and disease. Exp Eye Res. 1995; 61: 259-72.

27) Anderson DR. Correlation of the peripapillary anatomy with the disc damage and field abnormalities in glaucoma. Greve EL, Heijl A (Eds) Fifth International Visual Field Symposium: Volume 35 of the series Documenta Ophthalmologica Proceedings Series, 1982 The Hague, The Netherlands: Dr. W. Junk Publishers; 1983. p. 1-10.

28) Heijl A, Samander C. Peripapillary atrophy and glaucomatous visual field defects. Heijl A, Greve EL (Eds) Sixth International Visual Field Symposium: Volume 42 of the series Documenta Ophthalmologica Proceedings Series, 1984 Dordrecht, The Netherlands: Dr. W. Junk Publishers; 1985. p. 403-7.

29) Kawano J, Tomidokoro A, Mayama C, Kunimatsu S, Tomita G, Araie M. Correlation between hemifield visual field damage and corresponding parapapillary atrophy in normal-tension glaucoma. Am J Ophthalmol. 2006; 142: 40-5.

30) Geijssen HC. Studies on Normal Pressure Glaucoma New York, NY: USA: Kugler Publications; 1991.

31) Takumi T, Ito H, Anraku A, Takeyama A, Enomoto N, Ishida K, et al. Peripapillary atrophy and its relation to changes in the optic nerve head blood flow after usage of topical prostaglandin analogues. Eye. 2017; 34: 734-9.

32) Anderson DR, Patella VM. Automated Static Perimetry 2nd ed, St. Louis, MO, USA: Mosby; 1999.

33) Garway-Heath DF, Rudnicka AR, Lowe T, Foster PJ, Fitzke FW, Hitchings RA. Measurement of optic disc size: equivalence of methods to correct for ocular magnification. Br J Ophthalmol. 1998; 82: 643-9.

34) Ubuka M, Sugiyama T, Onoda Y, Shiba T, Hori Y, Maeno T. Changes in the blood flow of the optic nerve head induced by different concentrations of epinephrine in intravitreal infusion during vitreous surgery. Invest Ophthalmol Vis Sci. 2014; 55: 1625-9.

35) Kobayashi W, Kunikata H, Omodaka K, Togashi K, Ryu M,

Akiba M, et al. Correlation of papillomacular nerve fiber bundle thickness with central visual function in open-angle glaucoma. J Ophthalmol. 2015; 2015: 460918.

36） Sugiyama T, Araie M, Riva CE, Schmetterer L, Orgul S. Use of laser speckle flowgraphy in ocular blood flow research. Acta Ophthalmol. 2010; 88: 723-9.

37） Watanabe G, Fujii H, Kishi S. Imaging of choroidal hemodynamics in eyes with polypoidal choroidal vasculopathy using laser speckle phenomenon. Jpn J Ophthalmol. 2008; 52: 175-81.

38） Flamme J Jr, Orgul S, Costa VP, Orzalesi N, Krieglstein GK, Serra LM, et al. The impact of ocular blood flow in glaucoma. Prog Ret and Eye Res. 2002; 21: 359-93.

39） Werne A, Harris A, Moore D, BenZion I, Siesky B. The circadian variations in systemic blood pressure, ocular perfusion pressure, and ocular blood flow: risk factors for glaucoma? Surv Ophthalmol. 2008; 53: 559-67.

40） Hayashi K, Tomidokoro A, Lee KYC, Konno S, Saito H, Mayama C, et al. Spectral-domain optical coherence tomography of β-zone peripapillary atrophy: influence of myopia and glaucoma. Invest Ophthalmol Vis Sci. 2012; 53: 1499-505.